Eur. Phys. J. A **20**, 475–481 (2004)
DOI 10.1140/epja/i2003-10170-7

THE EUROPEAN PHYSICAL JOURNAL A

$\sigma(600)$ and background in $\pi\pi$ scattering

A.E. Kaloshin[a], V.M. Persikov, and A.N. Vall

Irkutsk State University, K. Marks Str. 1, 664003 Irkutsk, Russia

Received: 11 August 2003 / Revised version: 12 November 2003 /
Published online: 8 June 2004 –
Communicated by V.V. Anisovich

Abstract. We suggest a simple analytical description of the S-wave isoscalar $\pi\pi$ amplitude, which corresponds to a joint dressing of the bare resonance and background contributions. The amplitude describes well the experimental data on the δ_0^0 phase shift in the energy region below 900 MeV and has two poles in the Re $s > 0$ half-plane. Besides the well-known pole of the $\sigma(600)$-meson with Re $s \sim m_\pi^2$, there exists a more distant pole with Re $s \sim 0.6\,\mathrm{GeV}^2$. Our analysis is interpreted as an indication for the dynamical origin of the $\sigma(600)$ pole, while the second pole should be associated with lowest $q\bar{q}$ state.

PACS. 13.75.Lb Meson-meson interactions – 11.30.Rd Chiral symmerties – 14.40.Cs Other mesons with $S = C = 0$, mass < 2.5 GeV

1 Introduction

The properties of the lightest scalar meson $\sigma(600)$ are very important for the interpretation of a scalar family and details of the chiral-symmetry breaking. Appearance of a new experimental information and the theory development in the low-energy region generated an extensive discussion on this issue (see [1–5] and references therein). As for the existence of $\sigma(600)$, now it is an almost commonly accepted fact and this resonance is included back into Particle Data Group's tables.

There is a long story concerning the resonance interpretation of the S-wave amplitude $\pi\pi \to \pi\pi$ with isospin $I = 0$. One of the key moments of this story was a realization (see, *e.g.*, [6–8]) that apart from the resonance $\sigma(600)$ term there is an essential background contribution in this energy region. However, there is no evident recipe to divide the $\pi\pi$ amplitude into the resonance and background terms. The simplest and widely used method is the "adding in phase shift" of the resonance and background contributions (IA method in terminology of [7,8]):

$$\delta_0^0 = \delta^{\mathrm{R}} + \delta^{\mathrm{B}}. \tag{1}$$

The amplitude $\pi\pi \to \pi\pi$ in this case is

$$f_0^0(s) = \frac{e^{2i\delta_0^0} - 1}{2i\rho} = \frac{e^{2i\delta^{\mathrm{B}}} - 1}{2i\rho} + e^{2i\delta^{\mathrm{B}}} \cdot \frac{e^{2i\delta^{\mathrm{R}}} - 1}{2i\rho} = \frac{e^{2i\delta^{\mathrm{B}}} - 1}{2i\rho} + e^{2i\delta^{\mathrm{B}}} \cdot f^{\mathrm{Res}}(s). \tag{2}$$

The ansatz (1) may be derived from the summation of the loop contributions with some extra conditions [6]. To obtain the resonance parameters from the experimental data one needs an additional assumption about the form of the background contribution δ^{B}. The best way for a broad resonance is to determine its mass and the width from the pole position in the complex energy plane. However, only the resonance contribution $f^{\mathrm{Res}}(s)$ of the entire amplitude (2) can be continued into the complex energy plane. Thus it is possible to study the pole position but not the pole residue.

Other methods to describe the δ_0^0 phase shift, different from (1), either have so evident defects, or are much more complicated with many free parameters.

In this paper we suggest a very simple analytical parameterization for the $\pi\pi$ amplitude which allows us to continue it to the second Riemann sheet. The amplitude contains (in the spirit of the linear σ-model) two bare objects: the resonance and the background. The main idea is that a joint unitarization of two objects should be described correctly by the field theory methods. As concerns the form of a background contribution at the tree level, it can be modelled by a maximally simple method.

There are different ways to construct such analytical amplitude. We found the formalism of the unitary mixing to be the suitable one, the obtained amplitude is analytical and unitary automatically. Such construction is rather flexible which allows us to investigate some different physical situations.

Note that on the other hand the bare pole located at $s < 0$ may be considered as some effective cross-exchange and its value $m_2^2 \sim -m_\rho^2$, obtained from a fit, confirms

[a] e-mail: kaloshin@physdep.isu.ru

this interpretation. As compared with the standard N/D method our amplitude with two bare objects automatically has a zero, which is necessary to describe the S-wave low-energy data.

2 Formalism of the unitary mixing

If there exist n bare states with the same quantum numbers, then the dressing of their propagators should account also the mutual transitions between them. The process of joint dressing is described in this case by the system of Dyson-Schwinger equations:

$$\Pi_{ij}(s) = \pi_{ij}(s) - \Pi_{ik}(s)J_{kl}(s)\pi_{lj}(s), \qquad i,j = 1\dots n. \tag{3}$$

Here π_{ij} and Π_{ij} are bare and dressed propagators, respectively, J_{ij} are the self-energy contributions.

Let us consider the mixing of two resonances ($n = 2$) with one open intermediate state. In this case the solutions of (3) are

$$\Pi_{11} = \frac{D_2(s)}{D(s)}, \quad \Pi_{12} = \frac{J_{12}(s)}{D(s)}, \quad \Pi_{22} = \frac{D_1(s)}{D(s)}. \tag{4}$$

Here

$$D(s) = D_1D_2 - (J_{12}(s))^2,$$
$$D_1 = m_1^2 - s - J_{11}(s), \qquad D_2 = m_2^2 - s - J_{22}(s). \tag{5}$$

In the case of scalar resonances interacting with a pion pair, the loops are of the form[1]

$$J_{11}(s) = g_1^2 J(s), \quad J_{22}(s) = g_2^2 J(s), \quad J_{12}(s) = g_1 g_2 J(s). \tag{6}$$

$$J(s) = \frac{s-a}{\pi}\int_{4m_\pi^2}^{\infty} \frac{\mathrm{d}s'}{(s'-a)(s'-s)}\,\rho(s'), \tag{7}$$

where $0 < a < 4m_\pi^2$ is the subtraction point, g_i are the coupling constants and $\rho(s) = (1 - 4m_\pi^2/s)^{1/2}$.

The $\pi\pi$ amplitude

$$f = g_1^2\Pi_{11}(s) + g_2^2\Pi_{22}(s) + 2g_1g_2\Pi_{12}(s) = \frac{N(s)}{D(s)}, \tag{8}$$

where

$$D(s) = (m_1^2 - s)(m_2^2 - s) - J(s)N(s),$$
$$N(s) = g_1^2(m_2^2 - s) + g_2^2(m_1^2 - s). \tag{9}$$

It is evident that (8) satisfies the elastic unitary condition

$$\mathrm{Im}\ f = \rho|f|^2. \tag{10}$$

The above equations can be applied not only for the case of two resonances but also for the "resonance + background" situation, when one of the bare poles is located at $s < 0$. Right this situation arises for the S-wave $I = 0$ $\pi\pi \to \pi\pi$ amplitude. One can see from (9) that our amplitude is zero at the point

$$s_0^0 = (g_1^2m_2^2 + g_2^2m_1^2)/(g_1^2 + g_2^2), \tag{11}$$

which should be $s_0^0 \sim m_\pi^2$ to reproduce the Adler zero. So we have $m_2^2 < 0$ [2].

Let $m_2^2 < 0$ be the bare zero of function $D(s)$, which stays at the left of real axis after dressing. Then it is convenient to subtract the loop at this point:

$$D(s) = (m_1^2 - s)(m_2^2 - s) - (J(s) - J(m_2^2)) \times \left[g_1^2(m_2^2 - s) + g_2^2(m_1^2 - s)\right]. \tag{12}$$

Below we shall use the amplitude (8), (12) for the description of the experimental data. Here $m_1^2, g_1^2, m_2^2, g_2^2$ are free parameters. The background contribution at the tree level may be modelled by the pole or constant. It is sufficient for a successful description of the experimental data as is seen below.

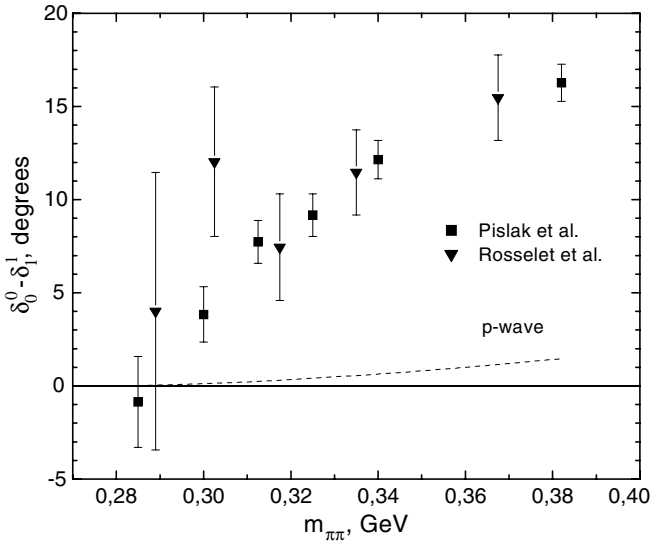

Fig. 1. Phase shift difference $\delta_0^0 - \delta_1^1$ from experiments on the K_{l4} decay.

3 Analysis of $\pi\pi$ data in region of $m_{\pi\pi} < 900$ MeV

In the near-threshold region we use the new data from the K_{l4} decay [10], which may be seen in fig. 1 in comparison with 1977 data [11]. We do not take into account the old data [11] as they have no practical effect on the fit. The measured value in the K_{l4} decay is the phase shift difference $\delta_0^0 - \delta_1^1$, thus we need an additional information on

[1] Note that we ignore the subtraction constants in the loops. As is shown in appendix A a subtraction polynomial in the loops can be removed by the redefinition of bare parameters.

[2] In spite of $m_2^2 < 0$, we keep using this notation to stress the presence of two objects in the amplitude. Note by the way that our amplitude (8) coincides, except for notations, with the amplitude of ref. [9], obtained from the low-energy bootstrap equations.

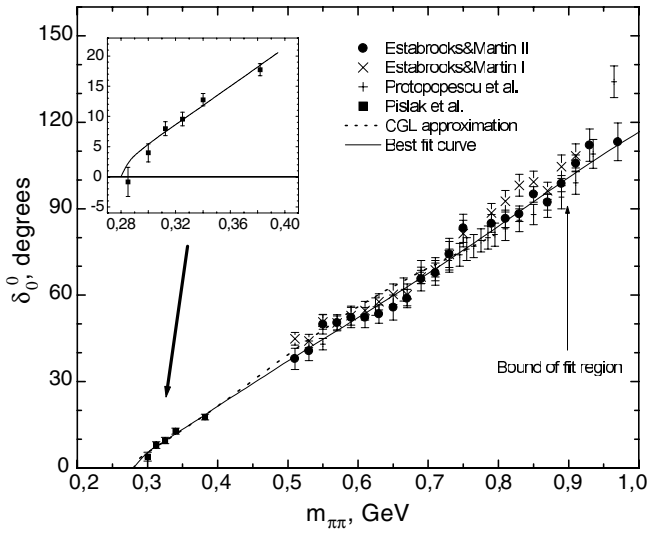

Fig. 2. Results of the fit of the $\pi\pi$ phase shift by the amplitude (12). The solid curve is the best fit to the data of the K_{l4} decay and EM II, its parameters can be seen in the first column of table 1.

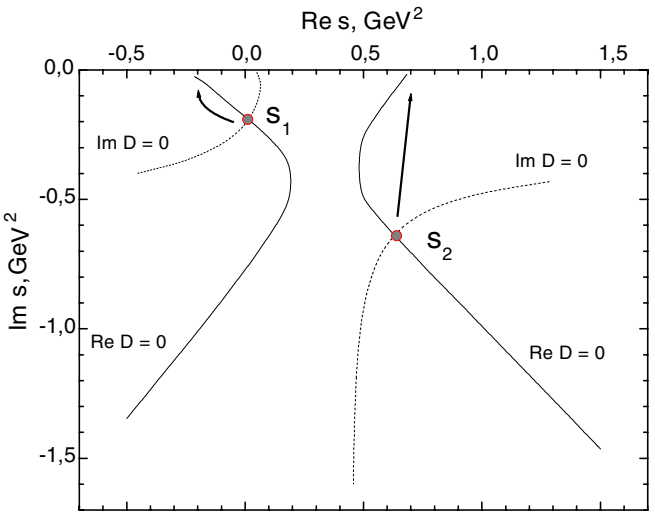

Fig. 3. Poles of the amplitude $\pi\pi \to \pi\pi$ with $J = I = 0$ on the second Riemann sheet at parameters (13). The arrows indicate the direction of the poles movement when the interaction is turned off.

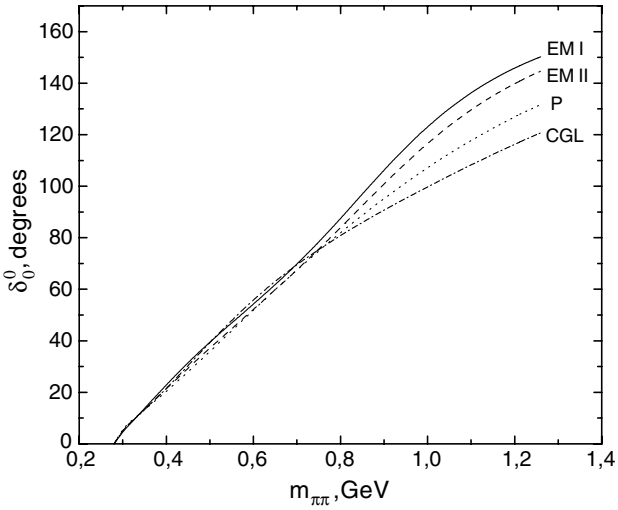

Fig. 4. Phase shifts corresponding to the different sets of parameters shown in table 1.

the P-wave. We use for this purpose the approximation of the solution of the Roy equations from ref. [12]. Fortunately, the δ_1^1 contribution is only about 1.5° at the end of the interval due to the P-wave threshold behavior, thus the uncertainty in δ_1^1 is negligible.

Our main purpose is the $\sigma(600)$-resonance, thus we restrict ourselves to the energy region $m_{\pi\pi} < 0.9$ GeV. It allows us to use the one-channel approach and not to take into account the $f_0(980)$ effect. In this region there exist different experiments and different analyses of the S-wave phase shifts, see recent reviews [13,14].

Below we use only classical partial analyses of Protopopescu *et al.* [15] from the $\pi^+ p \to \pi^+\pi^- \Delta^{++}$ reaction and the Estabrooks and Martin one of the CERN experiment [16] on $\pi^- p \to \pi^+\pi^- n$ (let us call their two solutions for the δ_0^0 phase shift EM I and EM II, respectively). Below we consider the mentioned experimental data on the δ_0^0 phase shift and find very similar conclusions. As an example we focus in more detail on the the EM II solution.

Figure 2 displays the results of joint fitting of K_{l4} data ($m_{\pi\pi} < 0.4$ GeV) and EM II data ($0.51 < m_{\pi\pi} < 0.9$ GeV). One can see that our amplitude (12) describes these data well.

Best-fit parameters are (in units of GeV^2)

$$\begin{aligned} m_1^2 &= 0.659 \pm 0.041, \qquad g_1^2 = 0.435 \pm 0.036, \\ m_2^2 &= -0.230 \pm 0.114, \quad g_2^2 = 0.177 \pm 0.067, \\ \chi^2/\mathrm{DOF} &= 17.7/21. \end{aligned} \tag{13}$$

Let us consider the zeros of function $D(s)$ at the second Riemann sheet[3]. The procedure of analytical continuation is described in appendix B. Figure 3 shows the zeros location in the complex s plane corresponding to the best-fit parameters (13). Let us stress that we find two zeros in the Re $s > 0$ half-plane.

Table 1 represents the results of the fit of the different low-energy data by our amplitude (12). All data sets lead to the solutions with two poles: close and distant[4].

In fig. 4 we compare phase shifts corresponding to different variants of table 1.

We can see that our simple model (12) corresponding to joint unitarization of two bare objects, one pole at $s < 0$ and another pole at $s > 0$, describes successfully the $\pi\pi$ phase shift δ_0^0 in the energy region below 900 MeV. We find

[3] The values of the bare parameters have rather limited meaning since they correspond to a given method of renormalization. However, the character of the pole movement is more meaningful, at least when the loop contributions do not dominate in amplitude.

[4] Our amplitude has a property $f(s^*) = f^*(s)$, thus we have a pair of the complex conjugate poles in the complex s plane. For definiteness we say about poles in the $Im\ s < 0$ half-plane.

Table 1. Results of the fit of the different sets of experimental data by our amplitude. m_i^2, g_i^2, s_i are in units of GeV^2. In the last column our parameterization is compared to the approximation of the phase shift from ref. [12] (Solution [17] of the Roy equations with use of scattering lengths from the two-loop chiral perturbation theory calculations.) Our phase shift practically coincides with the CGL approximation in this energy region.

K_{l4} + EM II $E < 0.9$ GeV	K_{l4} + EM I $E < 0.9$ GeV	K_{l4} + Protopopescu $E < 0.9$ GeV	CGL [12] $E < 0.8$ GeV
$m_1^2 = 0.659 \pm 0.041$ $g_1^2 = 0.435 \pm 0.036$ $m_2^2 = -0.230 \pm 0.114$ $g_2^2 = 0.177 \pm 0.067$ $\chi^2/\mathrm{DOF} = 17.7/21$	$m_1^2 = 0.586 \pm 0.025$ $g_1^2 = 0.382 \pm 0.020$ $m_2^2 = -0.113 \pm 0.053$ $g_2^2 = 0.116 \pm 0.030$ $\chi^2/\mathrm{DOF} = 22.6/21$	$m_1^2 = 0.794 \pm 0.114$ $g_1^2 = 0.598 \pm 0.151$ $m_2^2 = -0.580 \pm 0.405$ $g_2^2 = 0.422 \pm 0.331$ $\chi^2/\mathrm{DOF} = 5.3/19$	$m_1^2 = 0.845$ $g_1^2 = 0.779$ $m_2^2 = -0.573$ $g_2^2 = 0.548$ $\chi^2/\mathrm{DOF} = 0$
Poles: $s_1 = 0.015 - i\ 0.192$ $s_2 = 0.633 - i\ 0.630$	Poles: $s_1 = 0.045 - i\ 0.132$ $s_2 = 0.632 - i\ 0.533$	Poles: $s_1 = 0.055 - i\ 0.339$ $s_2 = 0.484 - i\ 1.020$	Poles: $s_1 = 0.104 - i\ 0.250$ $s_2 = 0.659 - i\ 1.620$

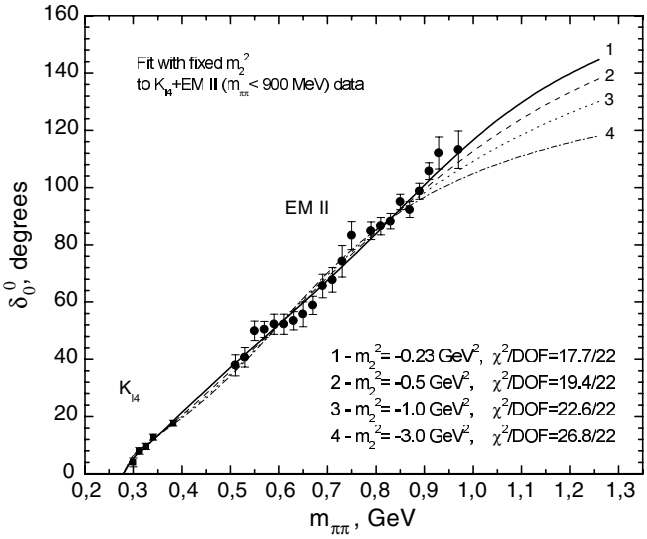

Fig. 5. Data fit at fixed value of the left pole m_2^2.

two poles in the complex s plane: one close to the origin with Re $s \sim m_\pi^2$ and the second one with Re $s \sim 0.6\,\mathrm{GeV}^2$. However, the behavior of the poles when the interaction is turned off $g_i^2 \to 0$ is rather unexpected (see fig. 3): the close pole traditionally identified with the $\sigma(600)$-meson moves to the negative-s region. While the second pole s_2 (most of previous analyses did not observe it) tends to the real axis above the threshold.

As an alternative we can investigate the case when the background has not bare pole. It corresponds to the joint dressing in the system "σ-pole + constant". For this purpose it is sufficient to put the value m_2^2 negative and large in our amplitude (12).

In fig. 5 the results of data fit with different m_2^2 values are shown. One can see that the experimental data prefer the rather close left pole $|m_2^2| < 0.6\,\mathrm{GeV}^2$.

Figure 6 illustrates the pole positions in the complex plane at value $m_2^2 = -1\,\mathrm{GeV}^2$ and their behavior when interaction is turned off. We observe that the behavior of poles has been changed as compared with $m_2^2 > -0.5\,\mathrm{GeV}^2$ case.

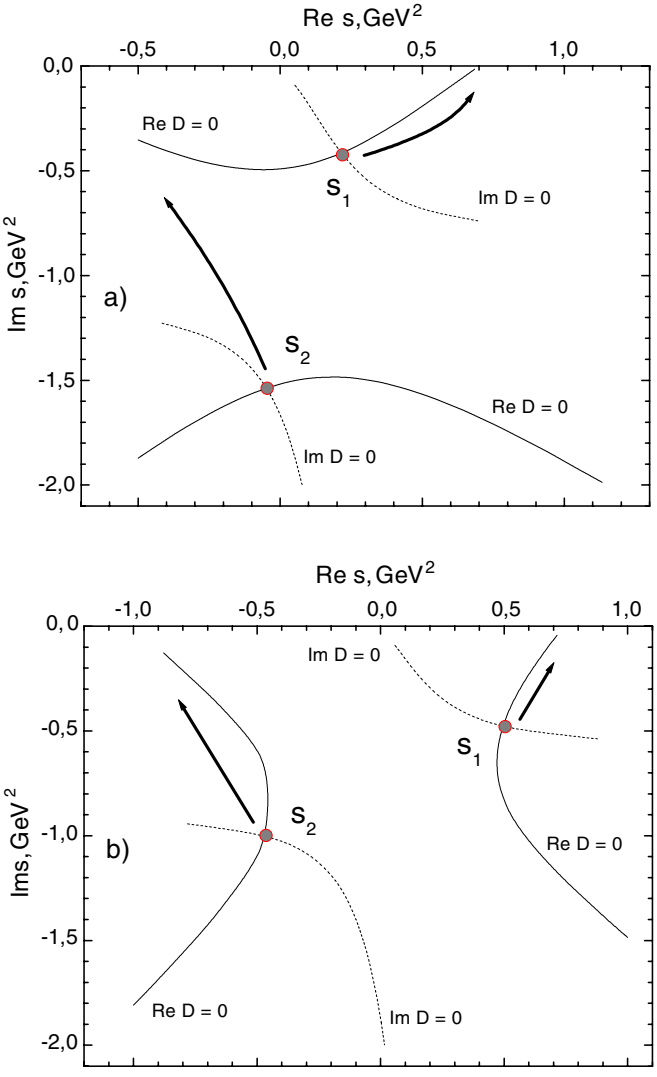

Fig. 6. a) Poles positions in the complex s plane at $m_2^2 = -1\,\mathrm{GeV}^2$ (fit of the data K_{l4} + EM II) and their movement at $g_i \to 0$; b) illustration of the poles movement. As compared with a) we slightly reduced the coupling constants $g_i^2 \to 0.75 g_i^2$ with the other parameters fixed.

4 Discussion

We found that the $\pi\pi$ phase shift δ_0^0 is well described by a simple analytical amplitude (12) in the energy region from the threshold up to 900 MeV. Our amplitude corresponds to a joint dressing of two bare objects: resonance and background contributions. Background can be modelled either by a pole with Re $s < 0$ or by a constant. As a next step one could investigate the more complicated background model: left pole + constant (just as in the linear σ-model). However, since our simple amplitude (12) provides a good description of the experimental data we suppose that the inclusion of new degrees of freedom has no meaning.

After the fit of the experimental data we found the presence of two complex poles at the second Riemann sheet: one close to the origin with Re $s_1 \sim m_\pi^2$ and the second one with Re $s_2 \sim 0.5$–$0.6\,\mathrm{GeV}^2$. The close pole was seen in most of the previous analyses of $\pi\pi$ scattering (its position is defined mainly by Adler zero) and it was associated with the lightest scalar meson $\sigma(600)$. Note that we approximated the background term at the tree level by some pole, physically it corresponds to the cross-exchange by the ρ- or σ-meson. The existing experimental data certainly prefer the pole form of the background as compared with the constant.

As for the behavior of the poles in the limit of $g_i \to 0$ we observe that only the distant pole goes to the real axis at positive s (see fig. 3). This fact holds true for all variants indicated in table 1. More detailed investigation shows that such a behavior changes with the m_2^2 value as is schematically illustrated in fig. 7. The experimental data on $\pi\pi$ scattering with energy below 900 MeV prefer the variant a), while the variant b) with $m_2^2 \sim -1\,\mathrm{GeV}^2$ also cannot be excluded (see fig. 5). For example, the found χ^2 values are $\chi^2/\mathrm{DOF} = 17.7/22$ for a) and $\chi^2/\mathrm{DOF} = 22.6/22$ for b) in one of the variants of the fit.

In view of the discussion [18–21,5] on whether the $\sigma(600)$ is an intrinsic state or it is dynamically generated, our results should be interpreted as an indication for a dynamical nature of the $\sigma(600)$. In this case the second pole should be associated with the intrinsic $q\bar{q}$ state having regard to the above remarks.

We suppose that the most interesting question is the meaning of the second pole s_2. It was seen only in a few previous analyses, *e.g.* in [2], where it was considered as an artefact since it was located out of the considered energy region. In our analysis with account of the much more exact data from the K_{l4} decay, this pole has moved to the lower value Re $s_2 \sim 0.6\,\mathrm{GeV}^2$. As for its imaginary part, it is rather uncertain (see table 1) and may be abnormally large for the resonance state. We suppose that the further fate of this pole may be solved by an analysis in the extended energy region.

In any case it is clear that in fact we have the joint complex "$\sigma(600)$ + Background + $f_0(980)$", which should be studied jointly and by the adequate methods.

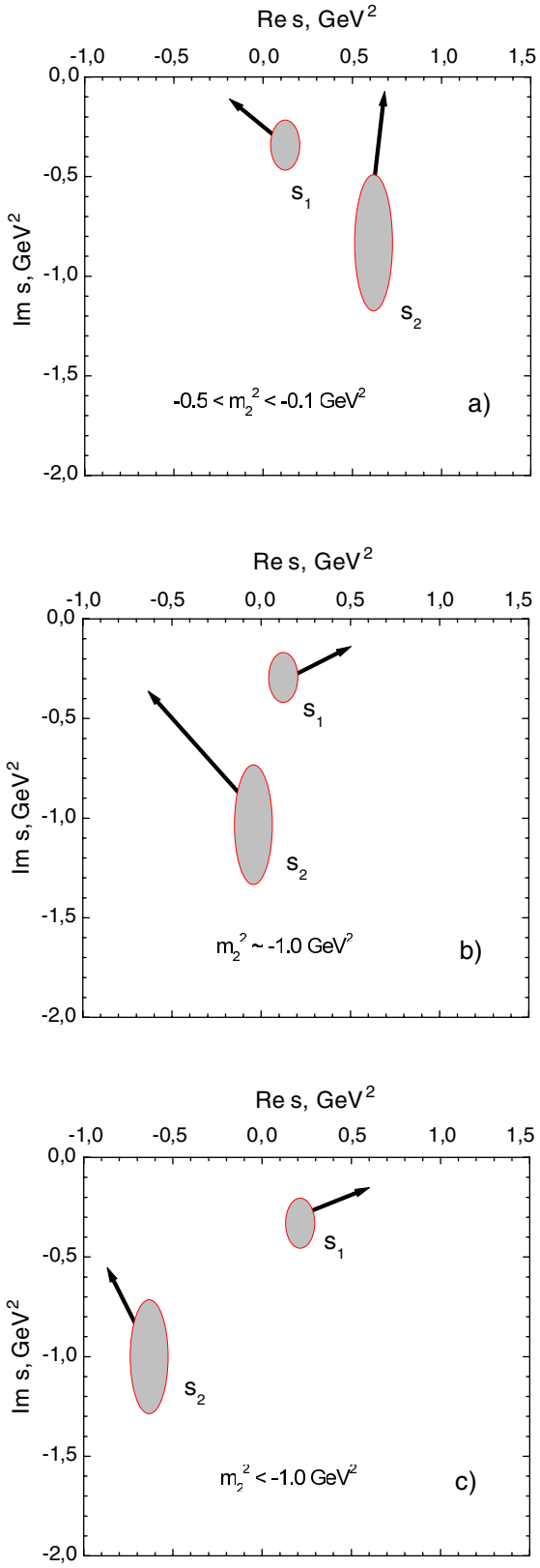

Fig. 7. Poles positions in the complex s plane and their movement at $g_i \to 0$ managed by the m_2^2 value. The variant a) is preferable by quality of the data description but b) also has an acceptable value of χ^2.

Appendix A. Reparameterization of hadron amplitude

Let us consider the unitary mixing of two bare poles with the presence of one intermediate state. We are interested in a number of independent parameters in the $\pi\pi \to \pi\pi$ amplitude. Let us write it in matrix form:

$$f = \left(g_1, g_2\right) \begin{pmatrix} \Pi_{11}, \Pi_{12} \\ \Pi_{21}, \Pi_{22} \end{pmatrix} \begin{pmatrix} g_1 \\ g_2 \end{pmatrix} \equiv g^T \cdot \Pi \cdot g \qquad \text{(A.1)}$$

Here Π is the symmetrical matrix of the propagator.

Let us start from the most general case when all loops have a subtraction polynomial of first degree[5].

$$J_{ij} = g_i g_j (P_{ij}(s) + J(s)) = g_i g_j (a_{ij} + b_{ij} s + J(s)), \quad \text{(A.2)}$$

where

$$J(s) = \frac{s-a}{\pi} \int_{4m_\pi^2}^{\infty} \frac{\mathrm{d}s'}{(s'-a)(s'-s)} \sqrt{\frac{s'-4m_\pi^2}{s'}}. \qquad \text{(A.3)}$$

Here a is subtraction point $0 < a < 4m_\pi^2$; for analytical continuation it is not convenient to subtract the integral at zero. There are ten parameters: bare masses m_1, m_2, coupling constants g_1, g_2 and 6 subtraction parameters in the loops.

We can perform a transformation of propagators and coupling constants, which does not change the amplitude:

$$\begin{aligned} f &= g^T \cdot S^{-1} S \cdot \Pi \cdot S^{-1} S \cdot g = g'^T \cdot \Pi' \cdot g', \\ \Pi' &= S \Pi S^{-1}, \qquad g' = Sg. \end{aligned} \qquad \text{(A.4)}$$

Let us make few transformations consequently:

1. Firstly by the orthogonal transformation

$$S = \begin{pmatrix} \cos\theta & \sin\theta \\ -\sin\theta & \cos\theta \end{pmatrix}$$

we delete the linear-on-s term in the non-diagonal loop: $b'_{12} = 0$.
2. Then by the scale transformation

$$\Gamma = \begin{pmatrix} \gamma_1 & 0 \\ 0 & \gamma_2 \end{pmatrix}$$

we make the coefficient at s in Π_{11}, Π_{22} by unity. After it any orthogonal transformation cannot generate again the linear-on-s term in the non-diagonal loop.
3. We use one more orthogonal transformation to delete a subtraction constant in the non-diagonal loop.
4. Finally, we can redefine the masses, absorbing the subtraction constants in the diagonal loops.

As a result we came to parametrization (4)-(7) which contains four parameters: masses and coupling constants.

[5] A higher degree of the polynomials leads to the domination of loops contributions at large s. It leads to the changing of the problem's index and to changing of number of poles as compared with the non-interactive case.

Appendix B. Analytical continuation of the loop

Let us consider the two-sheet analytical function:

$$\begin{aligned} F^{(n)}(s) &= i\sqrt{\frac{s-4m_\pi^2}{s}} = \\ & i\left|\frac{s-4m_\pi^2}{s}\right|^{1/2} \frac{e^{i\,\varphi_1/2}}{e^{i\,\varphi_2/2}} \cdot (-1)^{(n-1)}, \quad n = 1, 2. \end{aligned} \qquad \text{(B.1)}$$

The cuts are chosen from $-\infty$ to zero and from $4m_\pi^2$ to $+\infty$.

Let us write down the Cauchy theorem on the first Riemann sheet:

$$F^{(1)}(s) - F^{(1)}(a) = J^{(1)} + L(s)\,, \qquad \text{(B.2)}$$

$0 < a < 4m_\pi^2$,

$$\begin{aligned} J^{(1)} &= \frac{s-a}{\pi} \int_{4m_\pi^2}^{\infty} \frac{\mathrm{d}s'}{(s'-a)(s'-s)} \sqrt{\frac{s'-4m_\pi^2}{s'}}, \\ L(s) &= \frac{s-a}{\pi} \int_{-\infty}^{0} \frac{\mathrm{d}s'}{(s'-a)(s'-s)} \sqrt{\frac{4m_\pi^2-s'}{-s'}}. \end{aligned} \qquad \text{(B.3)}$$

One can see from (B.2) that continuation of the loop to the second Riemann sheet is performed as

$$\begin{aligned} J^{(2)} &= -F^{(1)}(s) - F^{(1)}(a) - L(s) = \\ & J^{(1)} - 2F^{(1)} = \\ & -J^{(1)} - 2(F(a) + L(s)). \end{aligned} \qquad \text{(B.4)}$$

The first expression seems the most convenient in numerical calculations.

References

1. P. Minkowski, W. Ochs, Eur. Phys. J. C **9**, 283 (1999).
2. V.V. Anisovich, V.A. Nikonov, Eur. Phys. J. A **8**, 401 (2000).
3. E. Klempt, in *Proceedings of Zuoz 2000, Phenomenology of Gauge Interactions*, edited by D. Graudenz, V. Markushin (PSI, Villigen, 2000) pp. 61-126.
4. N.A. Törnqvist, A.D. Polosa, Nucl. Phys. A **692**, 259 (2001).
5. E. van Beveren, F. Kleefeld, G. Rupp, M.D. Scadron, Mod. Phys. Lett. A **17**, 1673 (2002).
6. N.N. Achasov, G.N. Shestakov, Phys. Rev. D **49**, 5779 (1994).
7. S. Ishida *et al.*, Prog. Theor. Phys. **95**, 745 (1996); **98**, 1005 (1997).
8. K. Takamatsu, Prog. Theor. Phys. **102**, E52 (2001).
9. A.N. Vall, V.S. Dedushev, V.V. Serebryakov, Yad. Fiz. **17**, 126 (1973).
10. S. Pislak *et al.*, Phys. Rev. Lett. **87**, 221801 (2001).
11. L. Rosselet *et al.*, Phys. Rev. D **15**, 574 (1977).
12. G. Colangelo, J. Gasser, H. Leutwyler, Nucl. Phys. B **603**, 125 (2001).

13. V.V. Vereshagin, K.N. Mukhin, O.O. Patarakin, Usp. Fiz. Nauk **170**, 353 (2000).
14. F.J. Yndurain, *Low-energy pion physics*, arXiv: hep-ph/0212282, unpublished.
15. S.D. Protopopescu *et al.*, Phys. Rev. D **7**, 1279 (1973).
16. P. Estabrooks, A.D. Martin, Nucl. Phys. B **79**, 301 (1974).
17. B. Ananthanarayan, G. Colangelo, J. Gasser, H. Leutwyler, Phys. Rep. **353**, 207 (2001).
18. N.A. Törnqvist, M. Roos, Phys. Rev. Lett. **76**, 1575 (1996); **77**, 2333 (1996).
19. N. Izgur, J. Speth, Phys. Rev. Lett. **77**, 2332 (1996).
20. C.M. Shakin, Huangsheng Wang, Phys. Rev. D **63**, 014019 (2001).
21. M. Boglione, M.R. Pennington, Phys. Rev. D **65**, 114010 (2002).